Design and Test of Composite Relative Position Sensor for High-Speed Maglev Track Measurement System

Xiao-Bo Hong, Jun Wu, Yun-Zhou Zhang, and Yong-Xiang He

***Abstract*—A composite relative position sensor is studied in this paper. The sensor outputs square signal corresponding to the cogging cycle of long stator track, which is used as the spatial sampling pulse for high-speed maglev track measurement system, and also provides relative position, speed and direction information. The sensor uses only one group of detection coils to identify the cog and two photoelectric switches to identify the direction, thus effectively reducing the mass and size of the sensor. To make sure the sensor works normally when it vibrates vertically and passes through the track joint, the processing methods are given respectively. The factors that affect the dynamic response characteristics are analyzed and compared, it is considered that the discharge time constant of the demodulation has a great influence, and based on this, the detection speed limit of the sensor is calculated as 253km/h. The dynamic test is carried out by using the equivalent inductance method, and the results show that the sensor can respond normally and output the results correctly within the speed of 200km/h. In addition, it is demonstrated that the sensor can detect accurately within a detection distance of 22mm and a lateral deviation of ± 22mm through platform test.**

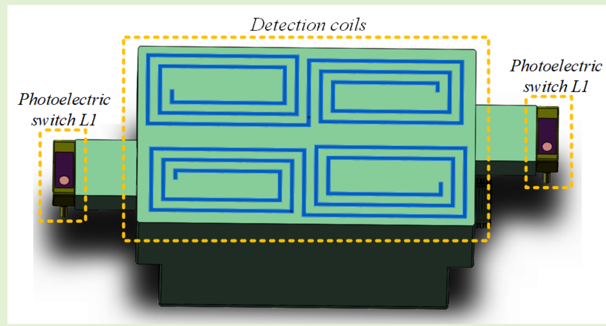

***Index Terms*—Maglev train, track measurement, relative position sensor, dynamic response, equivalent inductance method.**

I. Introduction

IN THE high-speed maglev track irregularity measurement system, track geometry and position data are collected at equal space intervals [1]. Since the maglev track itself is a linear synchronous motor, the stator of the track has a cogging structure, so the measuring point should always be located on the tooth surface. In addition, all the measured data should be linked to track mileage, and the data processing using mileage as the coordinate. Accurate location information can improve the positioning accuracy of defects, so as to facilitate maintenance. Therefore, a relative position detection sensor is needed to provide spatial sampling pulse, speed and position information for the irregularity detection system. In the field of wheel-rail transit, rotary encoder is widely used to provide position information in track measurement system [2]. However, for the high-speed maglev track measurement, the sampling pulse generated by the rotary encoder does not consider the cogging structure of the stator, which may cause the measurement point to deviate from tooth surface into cable trench, resulting in the measurement data mixed with abnormal values, and affecting the measurement accuracy of irregularity. Besides, due to the fluctuation of ± 2 mm in suspension (vertical) and guidance (transverse) when the train is running, the position sensor used must also have the characteristics of non-contact measurement. In addition, the width of the stator tooth is about 43mm. In order to ensure that the track measurement point is always on the tooth, the position detection error of the sensor should be less than the tooth width. Therefore, the position sensor for high-speed maglev track measurement must have the following requirements:

1. Accurately identify the tooth and slot of the track to generate a trigger pulse for sampling;
2. The maximum detection speed is 200km/h;
3. Overcome the influence of the train suspension fluctuation, allowing the detection distance to be 10-22mm;
4. Overcome the impact of the train guidance fluctuations, allowing the lateral position deviation to be to ±4mm;
5. Relative position detection error is within 43mm.

Manuscript received April 14, 2021; revised May 17, 2021; accepted May 23, 2021. Date of publication May 27, 2021; date of current version August 13, 2021. This work was supported by the National Key Research and Development Program of China under Grant 2016YFB1200602-40. The associate editor coordinating the review of this article and approving it for publication was Prof. Jean-Michel Redoute. *(Corresponding author: Jun Wu.)*

The authors are with the College of Intelligent Science, National University of Defense Technology, Changsha 410073, China (e-mail: hongxiaobo@163.com; wujun2008@nudt.edu.cn; zyz_ss1210@163.com; heyongxiang1995@163.com).

Digital Object Identifier 10.1109/JSEN.2021.3084369

The existing speed and position measurement device for maglev train include radar [3], cross induction loop [4]–[6], query transponder [7] and electromagnetic induction sensor [8].

As a special type of motor, position detection using Back EMF (electromotive force) is also used in high-speed maglev train, but this method can only be used at high speed, and cannot accurately identify the tooth and slot. At present, the relative position sensor (known as NUT in engineering, which is the abbreviation of *Nuten Messeinheit* in German) used in train operation control is just a kind of electromagnetic induction sensor, which realizes positioning through cogging detection and counting. This sensor can also be used in track measurement system. In addition, the output signal of the suspension gap sensor used in the train has cogging effect related to the stator structure [9], according to this feature, cogging signal can also be generated. The guideway monitoring system (GMS) used in Shanghai maglev line extracts spatial sampling pulse from the signal of gap sensor [10], [11].

NUT is one of the most important sensors on the train, it provides position information with accuracy of 4mm for the train traction system when the train is running at low speed, and provides cogging count at high speed [8]. The detection coil of NUT is an "8" shape with a differential construction to eliminate common-mode interference and improve coil sensitivity. NUT has two groups of coils, which differ by 1 / 4 of the cogging period along the longitudinal direction. The two coils cooperate to detect position, overcome the influence of suspended fluctuation and determine direction. When NUT works, the inner coil of the sensor emits high-frequency electromagnetic wave through the detection coil, thereby generating eddy current in the stator of the track. The eddy current field reacts on the detection coil, and the induced voltage and excitation voltage are superimposed on the detection coil. When the sensor moves, the equivalent inductance of the detection coil changes with the replacement of tooth and slot, generating a changing voltage signal. The cogging count can be obtained from the output signal of the sensor [14]. Since the cogging has a fixed period length (Δl=86mm), it is convenient to calculate the track mileage by counting. NUT was first invented in Germany and applied in TR series high speed maglev train, then inherited and developed by China till now. Literature [12] designed a relative position sensor for coil detection scheme, and literature [13] analyzed and optimized this sensor. Since then, adaptive filtering [14], [15], normalized levitation gap [16], tracking differentiator [17], [18] and Kalman filter [19] are used to process the sensor signal.

Although the positioning accuracy of NUT is high, its volume is large, and needs an additional control cabinet to process the sensor signal. For the track measurement system with independent function, the volume of the sensor is limited, and it does not need the high precision position requirement of the train control system. Thus the NUT is not suitable for track measurement system. It is necessary to design a compact position sensor according to the characteristics of the measurement system, which can be assembled with the track measurement system as a whole without the need of additional signal processing cabinet. Under the condition of volume limitation, the performance of the sensor can be optimized by optimizing the coil size, shape and layout. Reducing the volume of the sensor means that the coil size and layout must be changed. The problem studied in this paper is to maintain the best position detection accuracy and dynamic response characteristics under the condition of reducing the volume of the sensor, so that it can at least meet the requirements of high-speed magnetic levitation track measurement system.

In this paper, a composite sensor named (Hereinafter referred to as C-NUT, add *C* before NUT to represent the new type) is designed, which has the characteristics of small size and compact structure. It can complete the functions of position detection, speed calculation and direction discrimination. This sensor only uses one group of detection coils to identify the cogging structure, and generates the square-wave signal corresponding to the cogging cycle, which provides equal interval sampling pulse for the track measurement system. Two photoelectric switches with high frequency response are used to detect the presence or absence of cables on both sides of the stator and generate two square-wave signals, which are used to assist the detection coil to overcome the influence of suspension fluctuation and realize direction discrimination. This paper first introduces the structure design, working mode and signal processing flow of the sensor, expounds the detection principle of position, speed and direction, and on this basis, explains how to overcome the influence of vibration on the position detection accuracy, and the countermeasures when the sensor passes through the track joint. Then, the factors that affect the dynamic response of the sensor are analyzed. Finally, the equivalent inductance method is used to test the dynamic response, and the detection results of the sensor when the vertical and lateral position deviate are evaluated.

II. Sensor Design and Working Principle

C-NUT uses the same 8-shaped coil as NUT, which can eliminate the interference of external magnetic fields and improve the sensitivity, as shown in Fig. 1. But different from the former, C-NUT only uses one group of coils, and uses two high-frequency laser type photoelectric switches (L1 and L2) as auxiliary to realize position detection and direction discrimination. By reducing the number of coils, C-NUT avoids the parallel and staggered layout of two groups of coils, leaving space for a larger coil. Due to the change of coil size and layout, the overall dimension of C-NUT is greatly reduced compared with NUT. The compact sensor is suitable for installation in high-speed maglev track measurement system. Fig. 2 shows the newly developed track measurement system, C-NUT is installed on the upper part.

Fig. 3 shows the working scene of C-NUT. Laser type photoelectric switches are used to identify direction, and as auxiliary means of position detection. Compared with the detection coil, it has higher dynamic response characteristics. Two photoelectric switches are arranged on both sides of the sensor, the transverse distance is larger than the width of the stator, and the longitudinal distance is 1 / 4 of the cogging cycle. Two photoelectric switches generate two square-wave signals with phase difference of 90 degrees by detecting the presence or absence of cables on both sides of stator (hereinafter referred to as laser square-wave). The cable is embedded in the stator' slot, so there is no cable on both sides of the tooth. It can be considered that the characteristics of the

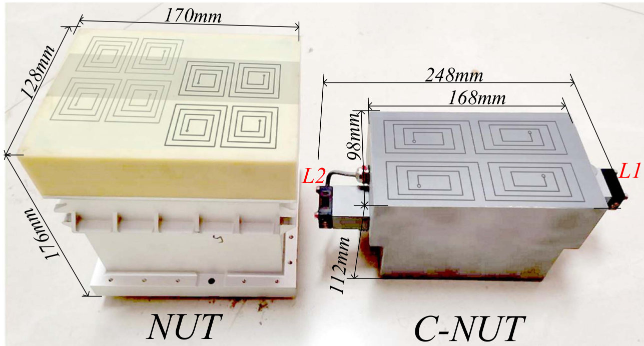

Fig. 1. Shape, dimension and coil layout of the two sensors(control cabinet is not included. Coils are packaged and actually invisible).

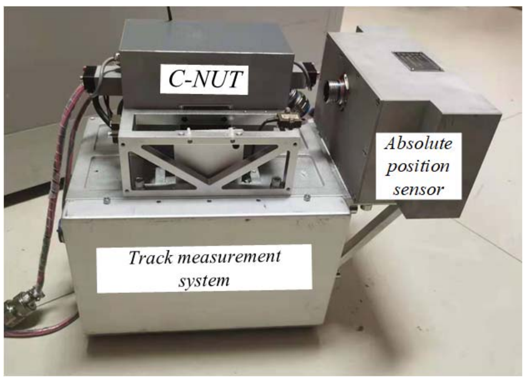

Fig. 2. Installation of C-NUT on track measurement system.

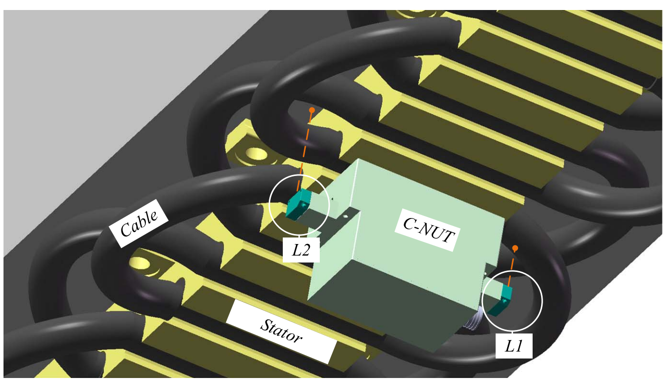

Fig. 3. Working scene of C-NUT.

cable layout correspond to the cogging structure, so the output signal of the photoelectric switch also contains the cogging information. It can be seen from the figure that the winding direction of the cable changes periodically, so the distance between adjacent cables on both sides of the stator is not consistent. The lateral position of the sensor changes due to the train guidance fluctuation, resulting in the duty cycle and phase change of the laser square-wave signal. Therefore, the laser square-wave cannot be used for position detection alone, but still be used for direction discrimination.

The circuit principle of C-NUT is shown in Fig. 4. The high-frequency carrier signal generated by crystal oscillator is fed to the resonant network after power amplification. The equivalent inductance of the detection coil will change due to the cogging structure, which will cause the resonance network to deviate from the resonance point. The resonant output signal carries the information of the cogging, and generates a square-wave pulse signal (hereinafter referred to as cogging square-wave) after demodulation, difference and comparison. The cogging square-wave and two laser square-waves are input into the digital unit at the same time, and finally the sampling pulse, relative position, direction and speed information are provided for the track measurement system.

The position detection methods used in NUT mainly include period prediction based method and signal sampling based method [20]. The signal sampling based method can obtain more accurate position information, but it needs two groups of detection coils to work together. However, C-NUT has only one group of coils, which is not suitable for this method. Because the position accuracy of the track measurement system is only 43mm, the period prediction based method can meet the requirements. This method predicts the current cogging cycle according to the historical information. and calculates the position according to the interpolation algorithm. Using the time data of the first three cogging cycle, the time length of the current cogging cycle is

$$T_e(n) = 3T(n-1) - 3T(n-2) + T(n-3) \tag{1}$$

When the positioning accuracy is $\Delta l/m$, a cogging cycle can be divided into m equal segments. The cogging cycle is very short, so it is considered that the time series of the sensor passing through m segments is approximately arithmetical sequence, and the difference is estimated as

$$\Delta t = \frac{T(n-1) - T_e(n)}{m^2} \tag{2}$$

In the n-th cogging cycle, the position update time of the i-th segment is as follows

$$T_e(n,i) = \frac{i}{m}T_e(n) + \frac{i(i-m)}{2}\Delta t \tag{3}$$

The velocity can be calculated by using the time length of the cogging cycle:

$$v = \frac{\Delta l}{T(n)} \tag{4}$$

The direction discrimination is obtained by logic judgment of two laser square-wave signals L1 and L2. The level of L2 is read at the rising edge of L1, as shown in Fig. 5. If L2 is low level, it is in forward operation, otherwise it is in reverse operation.

III. Processing of Special Working Conditions

As the key component of track detection system, C-NUT works on the train. Therefore, it is inevitable to face the following two working conditions: vibration and track joint, which will affect the accuracy of sensor position detection. Although the position accuracy requirement is not high, in order to improve the performance as much as possible, this paper presents the processing algorithm flow for these two conditions.

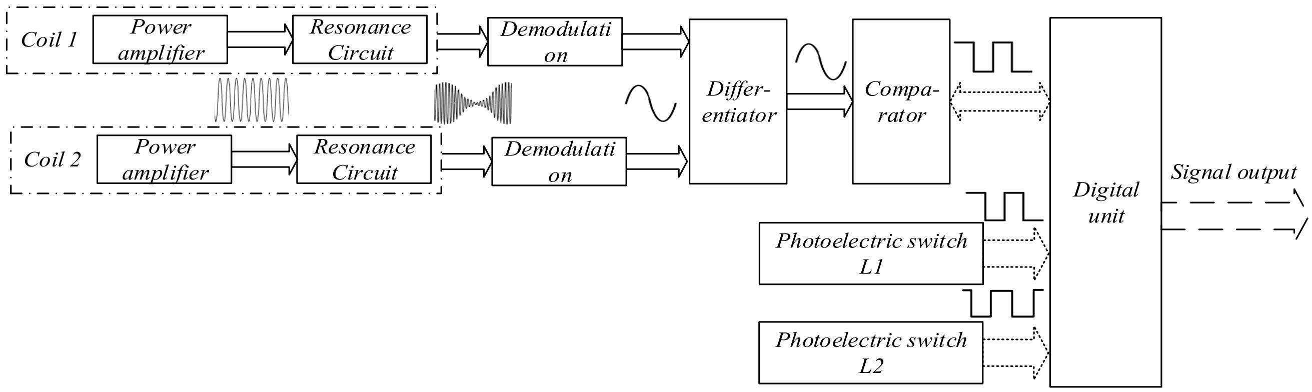

Fig. 4. Circuit principle of the sensor.

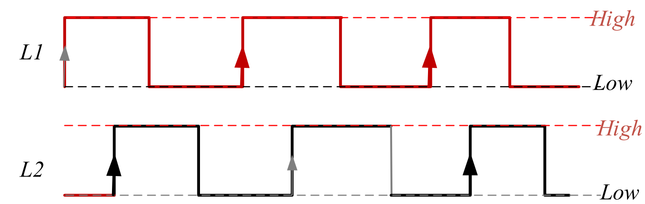

Fig. 5. Two laser square-wave signals in forward operation.

A. Vibration Processing Algorithm

When C-NUT is equipped on the train, the vertical detection distance will change due to the suspension fluctuation of the train, while the lateral detection position will deviate from the stator center due to the guidance fluctuation. Due to the change of winding direction of cables, the jumping time of laser square-wave changes during the lateral deviation, which may cause direction discrimination not timely, but has little impact on the track measurement. For vertical vibration, the detection distance of the sensor changes the amplitude and DC bias of the coil inductance, resulting in the change of the DC bias of the demodulation signal. Theoretically, the two detection coils and their resonant networks, processing circuits are identical, so the DC bias of the differential signal is zero. Due to the machining and layout factors, these two coils cannot be completely consistent, resulting in the DC bias of the differential signal is not zero. As shown in Fig. 6, there is a negative DC bias in the differential signal, and the cogging square-wave generated after zero crossing comparison jumps ahead of time, and the duty cycle of the signal decreases. For track measurement, the vertical vibration indirectly leads to the deviation of the actual measurement point from the expected position due to the use of the cogging square-wave as the sampling pulse.

To solve this problem, NUT uses a constant DC compensation method, whereby a DC bias is applied to the sensor during calibration so that the no-load differential voltage of the coil is zero. However, as the DC bias varies with the detection distance, the error cannot be completely eliminated by this method. In reference [13], a dynamic compensation method is proposed, which dynamically compensates differential signals by detecting the DC bias, thus effectively reducing errors. It is complicated to implement this method, in contrast, it is relatively easy to dynamically adjust the threshold voltage of comparator.

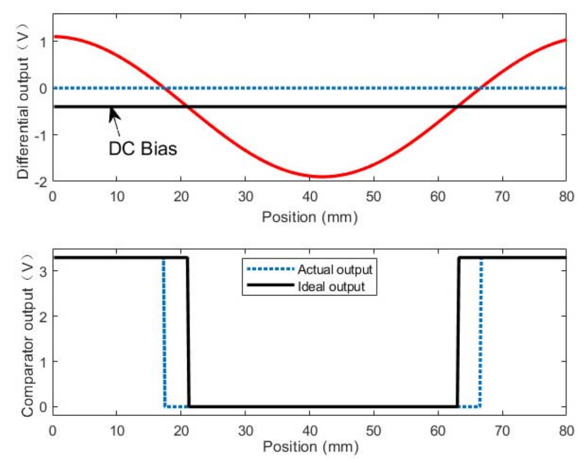

Fig. 6. The detection distance changes the phase and duty cycle of the cogging square-wave.

The DC bias can be obtained by sampling and calculating the differential signal with the jumping edge of the laser square-wave signal. The up and down jumping edges of laser square-wave L1 correspond to the crest and trough of differential signal respectively. Lateral deviation results in phase change of L1, and the sampling value of the corresponding differential signal will deviate from the crest and trough, which are recorded as S_p and S_v. The DC bias is obtained as follows

$$d = (S_p + S_v)/2 \tag{5}$$

The detected DC bias is directly used as the threshold voltage of comparator to ensure that the cogging square-wave can jump accurately and timely at different detection distances. Combined with the calculation method of relative position, speed and direction described in the previous section, the algorithm flow is shown in Fig. 7 below.

B. Track Joint Processing Algorithm

For the convenience of track installation and considering the influence of temperature deformation, there are joints between adjacent track beams with width of 80∼100 mm, as shown in Fig. 8. When the sensor passes by, it will cause the position calculation deviation, but the cogging count is normal. In addition, the width of track joint reaches 170mm at the end of turnout, which exceeds the length of the cogging cycle.

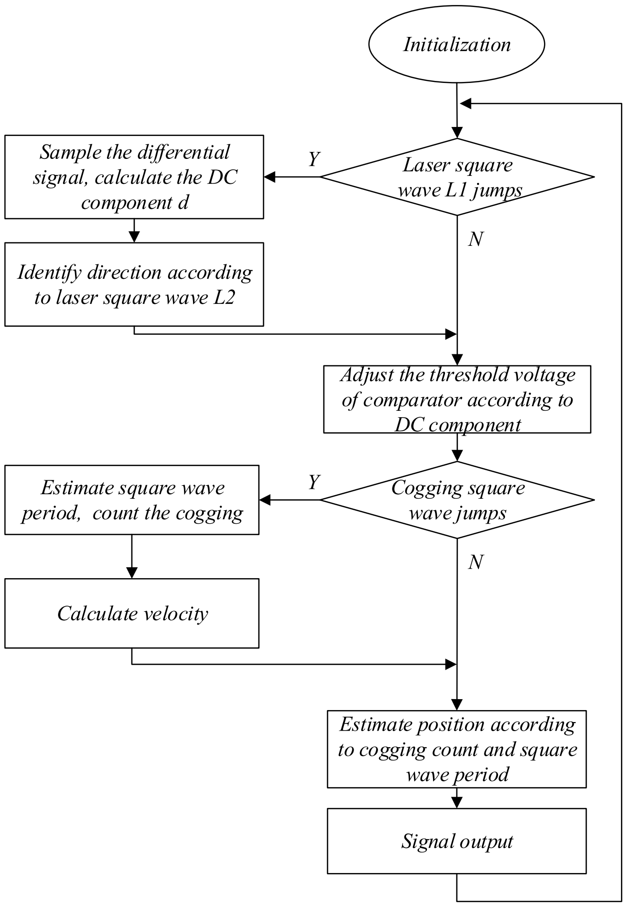

Fig. 7. Algorithm flow of vibration processing.

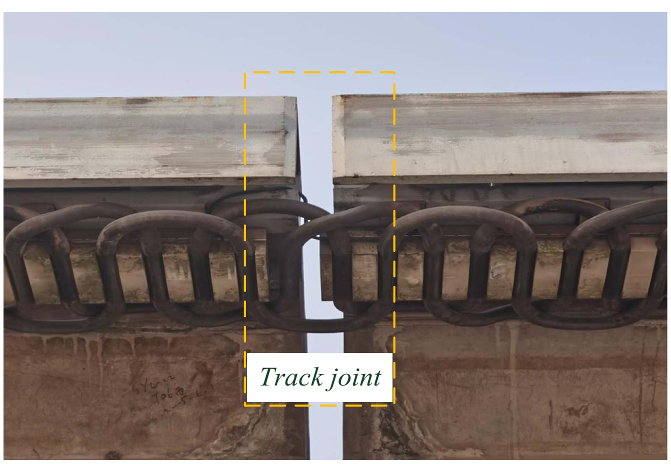

Fig. 8. Track joint.

In this case, the sensor will have a cogging count error and eventually lead to the deviation of mileage calculation.

Filtering, signal detection and dual sensor redundancy configurations are used in the NUT to keep the phase angle signal continuous when passing through the track joint. The track measurement system has no sampling points in the joint, and there is no requirement for the continuity of position information. Therefore, the processing can be simplified, only need to identify the track joint and estimate its width. In addition, due to the marked feature and fixed position in the line, absolute mileage information can be added to the track joint

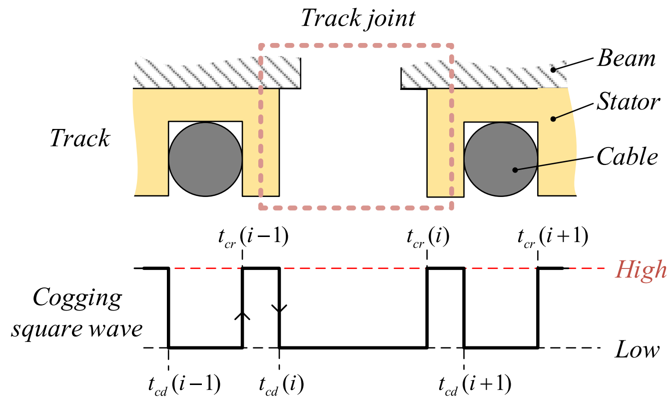

Fig. 9. Jumping time of cogging square-wave signal.

information, and the current absolute mileage can be obtained by identifying the track joint.

The width of the track joint is close to or exceeds the cogging cycle of the stator, and the tooth width of the stator end on both sides of the joint is only half of the normal width. Using this feature, the track joint can be identified, the joint width can be calculated according to the estimated velocity and the jumping time of the cogging square-wave signal, and the mileage of the current joint is obtained by matching the feature with the established database.

As shown in Fig. 9, the rising time of the cogging square-wave is t_{cr}, and the descending time is t_{cd}. The tooth width l_{dt} and slot width l_{ds} are estimated as follows

$$l_{dt} = v \cdot [t_{cd}(i) - t_{cr}(i-1)] \quad (6)$$

$$l_{ds} = v \cdot [t_{cr}(i) - t_{cd}(i)] \quad (7)$$

Compare the estimated tooth width and slot width with the standard cogging cycle Δl to determine whether the sensor is passing through the track joint. If so, record the current slot width as the joint width and count it. According to the width and counting information, the current absolute mileage is queried from the database, and the relative position is corrected accordingly. The algorithm flow is shown in Fig. 10. It should be noted that in the track measurement data processing, the mileage correction process is offline, so there is no real-time requirement for the implementation of the algorithm

IV. Analysis and Testing

A. Dynamic Response Analysis and Testing

The dynamic response of relative position sensor is an important parameter to evaluate its ability to respond to the change of position. NUT provides position information for train operation control, so it needs high response speed and position detection accuracy. In contrast, C-NUT provides 43mm spatial sampling pulse signal for the track measurement system, so the requirements for dynamic responses are greatly reduced. The dynamic response of C-NUT shows that the output signal lags behind. For the track measurement system, the trigger delay should be limited to half a cogging cycle, i.e. C-NUT must provide a sampling pulse in time within a tooth width, otherwise the sampling point of the system will deviate from the tooth surface, resulting in the failure of the detection data.

The factors that affect the dynamic responses of the sensor include resonance network, demodulation circuit and eddy

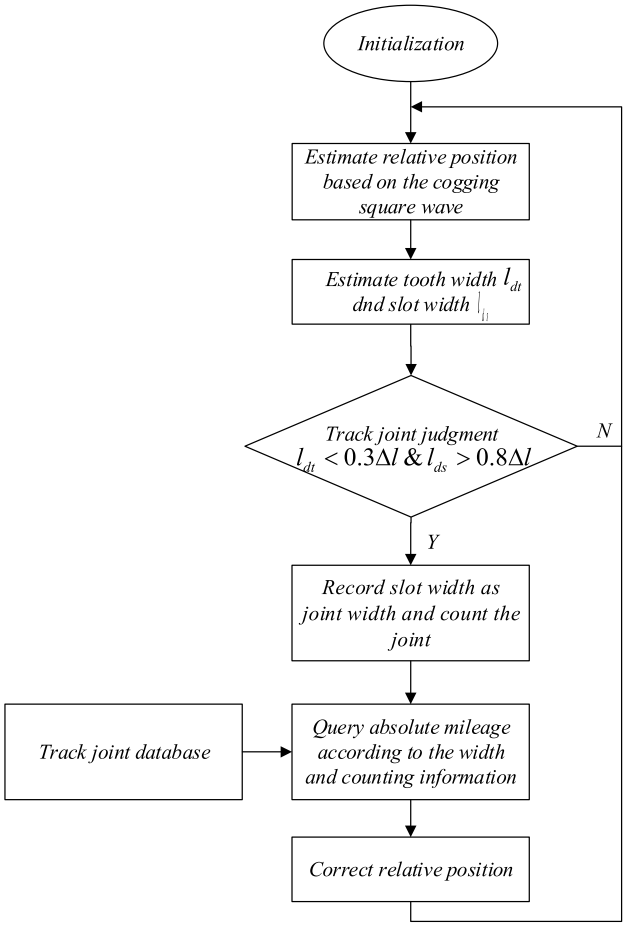

Fig. 10. Algorithm flow of track joint processing.

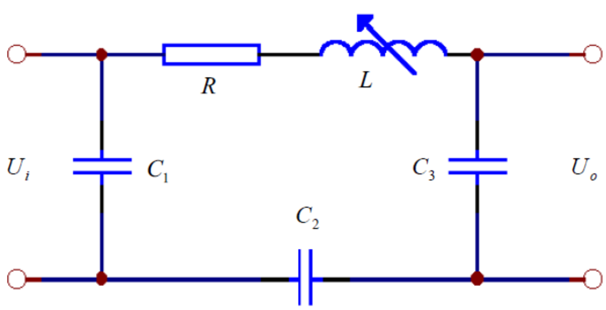

Fig. 11. Equivalent circuit of resonant network.

current loop. Among them, the eddy current loop is the electromagnetic coupling relationship between the detection coil and the measured track, which has little influence on the dynamic responses and can be ignored. Therefore, only the influence of resonance network and demodulation circuit on the dynamic response is considered. The resonant network is LC oscillation circuit, which can be equivalent to the resonant circuit with input voltage source, as shown in Fig. 11.

The frequency of the oscillation circuit is mainly determined by the coil resistance R, coil inductance L, capacitor C_1, C_2 and C_3. U_1 Is the feedback input voltage at resonance, and U_o is the output voltage. When resonant, the current of the two branches is equal, and the phase difference is π. From Kirchhoff voltage law

$$LC_3\frac{d^2U_o}{dt^2}+RC_3\frac{dU_o}{dt}+\frac{C_3}{C}U_o=0 \tag{8}$$

The characteristic polynomial is

$$LCs^2+RCs+1=0 \tag{9}$$

where, $C=\frac{C_1C_2C_3}{C_1C_2+C_2C_3+C_3C_1}$

The oscillator parameters satisfy $(RC)^2-4LC<0$ and the characteristic root is

$$s_{12}=-\frac{R}{2L}+j\sqrt{\left|(\frac{R}{2L})^2-\frac{1}{LC}\right|} \tag{10}$$

The zero input response of the equivalent circuit is an attenuated sinusoidal oscillation, and the attenuation time constant is the delay time constant of the resonant network under high frequency AC excitation. The time constant τ_0 and frequency f of the equivalent circuit are

$$\tau_0=\frac{2L}{R},\ f=\frac{1}{2\pi\sqrt{LC}} \tag{11}$$

The demodulation circuit consists of a charging circuit and a discharging circuit, which detects the peak voltage of AC signal by fast charging and slow discharging. The charging circuit consists of signal source internal resistance r, demodulation diode forward conduction resistance R_d and demodulation capacitance C_i; discharge circuit consists of demodulation load resistance R_i and demodulation capacitance C_i. The discharge time constant τ_2 is much larger than the charging time constant τ_1 because R_i is much larger than the input resistance $R'(R'=R_d+r)$. These two time constants are calculated as

$$\tau_1=R'C_i,\ \tau_z=R_iC_i, \tag{12}$$

The measured parameters of the sensor are $L=57.4\mu H$, $R=9.67\Omega$, $C_i=0.01\mu F$, $R_i=60k\Omega$, $R'=1k\Omega$ and the calculable time constants are respectively $\tau_0=0.012ms$, $\tau_1=0.01ms$, $\tau_z=0.6ms$. In addition, as the photoelectric switch is an auxiliary means of sensor position detection, special requirements should be made for its dynamic response characteristics. In c-nut, laser switch is a mature product on the market, and its response time is about $0.25ms$. After comparing those delay time, it is considered that the time constant τ_2 of the demodulation circuit has a great influence on the dynamic response of the sensor.

Considering that the response delay of C-NUT causes the position deviation of sampling points in the track measurement system, based on the above time constant, the maximum applicable detection speed of C-NUT is obtained as follows

$$v_H=\frac{\Delta l/2}{\tau_2+\tau_1}\approx 253km/h \tag{13}$$

At present, the existing dynamic response test methods of relative position sensor are mechanical method and equivalent inductance method [21]. The mechanical method can only obtain the dynamic responses in the range of tens of Hertz, but it is difficult to measure the frequency characteristics of hundreds to thousands of Hertz, so this paper test the dynamic response by using the equivalent inductance method.

The essence of the sensor to detect the change of the cogging is the signal modulation and demodulation based on the high frequency carrier. The induced voltage caused by cogging change is modulation signal, while the high frequency constant amplitude signal generated by resonant network is

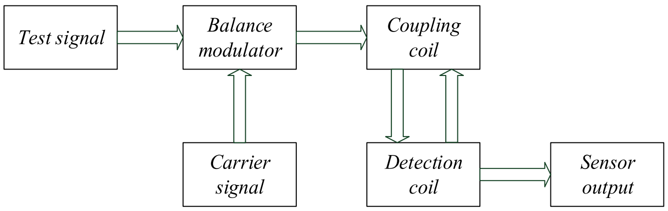

Fig. 12. Principle of equivalent inductance method.

TABLE I
RESULTS OF DYNAMIC RESPONSE TEST

Detection speed (*km/h*)	0.3	3	15	31	93	155	217
Frequency of test signal (*Hz*)	1	10	50	100	300	500	700
Frequency of output signal (*Hz*)	1	10	50	100	300	500	700

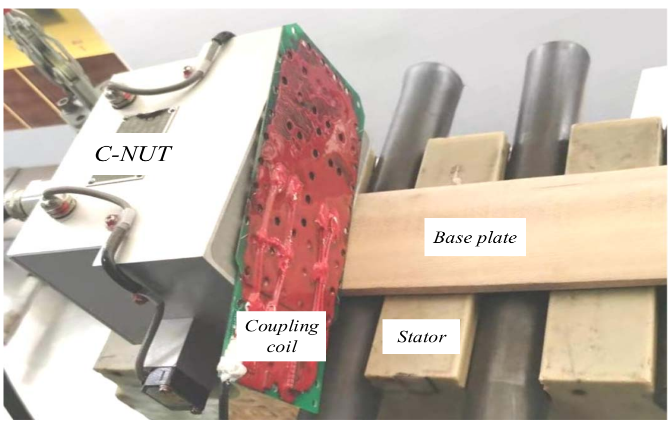

Fig. 13. Dynamic response testing of C-NUT.

carrier wave. The equivalent inductance method is based on the principle of modulation and demodulation, and its principle is illustrated in Fig. 12. The test signal is modulated to the high-frequency fundamental wave, and applied to the coupling coil to generate the simulated eddy current electromagnetic field. The induced voltage is generated in the detection coil of the sensor. In this way, the output of the sensor reflects the low frequency test signal.

As shown in Fig. 13, the coupling coil is close to the detection surface of C-NUT. The test signal is a low frequency square-wave signal, which is modulated to excite the analog coil. The frequency range of the test signal is 0-700Hz, corresponding to the detection speed of 0-217km/h. The test results are shown in Table I. The detection circuit of the sensor outputs the signal with the same frequency as the square-wave, indicating that the sensor can respond normally and output the results correctly when the speed is in the range of 200km/h.

B. Position Deviation Testing

It can be seen from the above analysis that the suspension fluctuation of the train leads to the change of the detection distance of C-NUT, and the guidance fluctuation leads to the lateral deviation of C-NUT relative to the stator. These two situations may affect the detection results of the sensor, so it is necessary to test C-NUT in the case of detection position deviation. As shown in Fig. 14, the detection distance is adjusted by changing the base plate with different thickness, and the deviation between the sensor and the stator center line is changed by moving the sensor horizontally. When the voltage of the sampling pulse output from the sensor U_{sam} is greater than 22V, it means that sensor is facing the tooth surface, while the voltage less than 0.6V indicates that the sensor is facing the slot surface. While the direction signal voltage U_{dir} greater than 22V means the detection direction is forward, and less than 0.6V is the reverse detection. The test results show that the sensor can output accurately when the detection distance is within 22mm. The sampling pulse is wrong when the detection distance is more than 22mm, but the direction signal is correct.

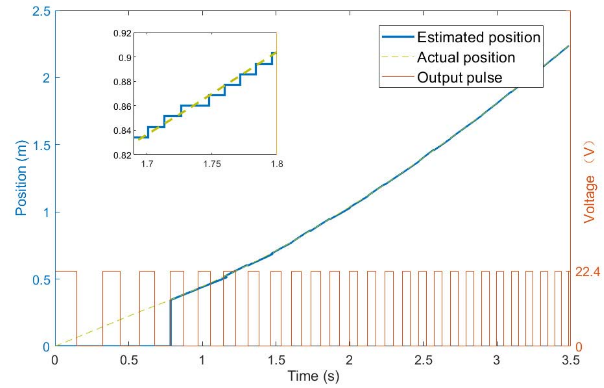

Fig. 14. Position detection results.

TABLE II
RESULTS OF POSITION DEVIATION TESTING

Lateral deviation (*mm*)		Detection distance (*mm*)				
		10	14	18	22	26
-22	U_{sam} at tooth surface (V)	22.4	22.4	22.4	22.4	0.45
	U_{sam} at slot surface (V)	0.45	0.45	0.45	0.45	0.45
	U_{dir} (V)	22.4	22.4	22.4	22.4	22.4
	Conclusion	OK	OK	OK	OK	ERROR
0	U_{sam} at tooth surface (V)	22.4	22.4	22.4	22.4	0.45
	U_{sam} at slot surface (V)	0.45	0.45	0.45	0.45	0.45
	U_{dir} (V)	22.4	22.4	22.4	22.4	22.4
	Conclusion	OK	OK	OK	OK	ERROR
22	U_{sam} at tooth surface (V)	22.4	22.4	22.4	22.4	0.45
	U_{sam} at slot surface (V)	0.45	0.45	0.45	0.45	0.45
	U_{dir} (V)	22.4	22.4	22.4	22.4	22.4
	Conclusion	OK	OK	OK	OK	ERROR

C. Position Detection Error Testing

Whether C-NUT can be used in maglev track measurement system needs to test its position detection error. The test method is to synchronously move C-NUT and cable displacement sensor, and record the time period of the output pulse of the C-NUT, which is used as the trigger pulse for sampling the cable displacement sensor. The accuracy of position obtained by cable displacement sensor is relatively high, which can be regarded as the actual position. The position of NUT was estimated by pulse period and compared with the actual position. The experimental record is shown in Fig. 13.

It can be seen from the figure that the estimated position of c-nut in long distance basically coincides with the actual position. The local enlarged image shows the change of the estimated position and the actual position in a cogging period. The estimated position is updated every 0.1s, and fluctuates around the actual position. The deviation between these two position curves indicates the sensor error, with a maximum error of approximately 10mm. Because the initialization of the position estimation algorithm needs to use the period of the first three pulses, the estimated position can only be obtained in the fourth cogging cycle. For maglev operational motion control is not acceptable, but for track measurement, this detection accuracy is more than enough. In addition, due to the limitation of test conditions, the movement speed of C-NUT in this test was only about 0.6m/s, so this paper only presented the position detection results under low speed test. Test at high speed will be carried out in the next stage.

Through the above dynamic response test, position deviation test and position detection error test, it is proved that C-NUT fully meets the detection speed of 200km/h required by the track measurement system, withstands the levitation and guidance fluctuation of maglev train, and the position detection error is less than 43mm.

V. Conclusion

In order to meet the spatial sampling pulses needed by high-speed maglev track measurement system and provide relative position, velocity and direction information, a composite position sensor is designed in this paper. It is small and compact, and can be installed in combination with the track measurement system as a whole;

C-nut uses only one set of detection coils, which allows configuration of larger coil sizes. The cogging structure of the stator on the track is identified by the detection coil, and the corresponding cogging square-wave is generated. Two photoelectric switches are used to detect the presence of cables outside the stator, and two laser square-wave signals with phase difference of 90 ° are generated for direction discrimination. The differential signal of two detection coils is sampled and the DC bias is calculated by using the jump edge of the laser square-wave, and the threshold voltage of the comparator is adjusted accordingly to overcome the influence of the vertical vibration on the position detection accuracy;

The time constant of demodulation circuit has a large impact on the dynamic response of the sensor. Considering the influence of response delay on the track measurement system, the maximum applicable detection speed of C-NUT is 253 km/h;

The dynamic responses of C-NUT are tested by the equivalent inductance method, the results show that the sensor can respond normally and output the results correctly within the speed of 200 km/h. In addition, the sensor is tested in vertical and lateral position deviation, and the results show that the sensor can detect accurately when the detection distance is within 22mm and the lateral offset is ± 22mm. Besides, the estimated position error of the sensor can reach 10mm at low speed, which is enough to meet the requirements of the track measurement system.

References

[1] J. Lee, J. Jo, Y. Han, C. Lee, and Y. Sun, "A study on the sensor applications for position detection and guideway monitoring in high speed maglev," *Mod. Mech. Eng.*, vol. 4, no. 4, pp. 165–174, 2014.

[2] Z. Liu, C. Dong, Y. Pei, and J. Kong, "Online rail straightness measurement based on parallel computing," in *Proc. 3rd Int. Conf. Mater., Mech. Manuf. Eng.*, Guangzhou, China, 2015, pp. 1112–1115.

[3] D. Zhang, Z. Long, and C. Dai, "Design and realization of a novel position-and-speed measurement system with communication function for the low-speed maglev train," *Sens. Actuators A, Phys.*, vol. 203, pp. 261–271, Dec. 2013.

[4] W. Nai, X. Li, Y. Yu, and S. Wang, "Study on absolute positioning technique for medium-low speed maglev train based on cross coding inductive loop wire," in *Proc. 2nd Int. Conf. Adv. Mech. Eng. Ind. Informat. (AMEII)*, Hangzhou, China, 2016, pp. 622–627.

[5] W. Nai, Y. Chen, Y. Yu, F. Zhang, D. Dong, and S. Wang, "Design and optimization of positioning and speed measuring system in engineering application for medium-low speed maglev train," in *Proc. IEEE Int. Conf. Veh. Electron. Saf. (ICVES)*, Beijing, China, Jul. 2016, pp. 1–5.

[6] X. Jiang, W. Nai, A. Yilixiati, Y. Yu, S. Wang, and D. Dong, "A train positioning mechanism for medium-low speed maglev train based on parity check cross coding inductive loop wire," in *Proc. 3rd IEEE Int. Conf. Control Sci. Syst. Eng. (ICCSSE)*, Beijing, China, Aug. 2017, pp. 269–272.

[7] J. Wang, D. Ni, and K. Li, "RFID-based vehicle positioning and its applications in connected vehicles," *Sensors*, vol. 14, no. 3, pp. 4225–4238, Mar. 2014.

[8] G. Luo, C. Dai, L. Tan, and Z. Long, "Research on suspension height and displacement decoupling of relative position detection sensor for high-speed maglev train," in *Proc. 9th Int. Conf. Intell. Hum.-Mach. Syst. Cybern. (IHMSC)*, Hangzhou, China, Aug. 2017, pp. 346–350.

[9] Y. Jing and J. Xiao, "Study on slot effect compensation method for gap sensor of high-speed maglev train," (in Chinese), *Transducer Microsyst. Technol.*, vol. 32, no. 4, pp. 16–18, Jan. 2013.

[10] W. Nieters, "Guideway monitoring during operational use on the first transrapid line in Shanghai," in *Proc. Int. Conf. Maglev*, Shanghai, China, 2004, pp. 480–485.

[11] W. Nieters and J. Shao, "Long wave guideway contour monitoring," in *Proc. Int. Conf. Maglev*, San-Diego, CA, USA, 2008. [Online]. Available: http://www.maglev.ir/eng/documents/papers/conferences

[12] Y. Sun, L. Li, and J. Wu, "Design of relative position detection sensor for high speed maglev train," (in Chinese), *Process Autom. Instrum.*, vol. 29, no. 7, pp. 63–65, 2008.

[13] H. Ning, X. Song, L. Zhiqiang, and Z. Jingnan, "Analysis and optimal design of relative position detection sensor for high speed maglev train," in *Proc. 5th Int. Conf. Intell. Comput. Technol. Autom.*, Zhangjiajie, China, Jan. 2012, pp. 89–93.

[14] S. Xue, N. He, and Z. Long, "Electromagnetic field analysis and modeling of a relative position detection sensor for high speed maglev trains," *Sensors*, vol. 12, no. 5, pp. 6447–6462, May 2012.

[15] C. Dai, S. Xue, and Z. Long, "The signal disposal of position and speed detection sensors based upon long stators for maglev train," (in Chinese), *Chin. J. Sens. Actuators*, vol. 22, no. 6, pp. 822–826, 2009.

[16] J. Wu, W. Zhou, and L. Li, "Research on speed and position detection system of high speed maglev train," (in Chinese), *J. Nat. Univ. Defense Technol.*, vol. 33, no. 1, pp. 109–114, 2011.

[17] F. Dou, H. He, and Y. Xie, "Research on the signal processing of position and speed detection system in maglev train based on tracking differentiator," (in Chinese), *J. China Railway Soc.*, vol. 38, no. 1, pp. 81–85, 2016.

[18] D. Fengshan, W. Zhiqiang, H. Hongli, and L. Zhiqiang, "On realization of signal processing based on tracking-differentiator for maglev train," in *Proc. 34th Chin. Control Conf. (CCC)*, Hangzhou, China, Jul. 2015, pp. 4646–4650.

[19] C. Dai, G. Luo, and Z. Long, "A signal process algorithm of relative position detection sensor for high speed maglev trains based on KF-UKF," in *Proc. IEEE Int. Conf. Signal Process., Commun. Comput. (ICSPCC)*, Xiamen, China, Oct. 2017, pp. 1–6.

[20] L. Lu and J. Wu, "Research and design of a position detection sensor for high speed maglev train," (in Chinese), *J. Sens. Actuators*, vol. 20, no. 7, pp. 1510–1513, 2007.

[21] S. J. Fan, J. Wu, L. Li, and W. S. Chang, "The measurement method of dynamic response based on modem," (in Chinese), *J. Nat. Univ. Defense Technol.*, vol. 27, no. 3, pp. 58–61, 2005.